Available online at www.sciencedirect.com
SCIENCE DIRECT
Quaternary Research 65 (2006) 293 – 307
QUATERNARY RESEARCH
www.elsevier.com/locate/yqres

Soil-forming rates and processes on Quaternary moraines near Lago Buenos Aires, Argentina

Daniel C. Douglass [a,*], James G. Bockheim [b]

[a] Department of Geology and Geophysics, University of Wisconsin, Madison, 1215 West Dayton Street, Madison, WI 53706, USA
[b] Department of Soil Science, University of Wisconsin, Madison, 1525 Observatory Drive, Madison, WI 53706-1299, USA

Received 25 January 2005
Available online 2 November 2005

Abstract

Thirty-four pedons on four moraine groups spanning the last 1 myr are used to investigate mechanisms and rates of soil development in Santa Cruz province, Argentina. All soils are coarse-loamy, mesic, Typic Haplocalcids or Calcic Haploxerolls occurring under short grass-shrub steppe, in a semi-arid climate. The dominant soil-forming processes are the accumulation of organic matter, carbonate, and clay-sized particles. Organic carbon accumulates rapidly in these soils, but significantly higher amounts in the oldest two moraine groups are likely the result of slight differences in soil-forming environment or grazing practices. Accumulation rates of carbonate and clay decrease with age, suggesting either decreased influx in the earliest part of the record or attainment of equilibrium between influx and loss. There are no changes in soil redness, and preservation of weatherable minerals in the oldest soils indicates there is little chemical weathering in this environment. Measured dust input explains the accumulation of both clay and carbonate. We present a carbonate cycling model that describes potential sources and calcium mobility in this environment. Calibration of rates of soil formation creates a powerful correlation tool for comparing other glacial deposits in Argentina to the well-dated moraines at Lago Buenos Aires.

Keywords: Argentina; Patagonia; Soil geomorphology; Soil development; Melanization; Calcification; Clay accumulation; Eolian dust; Soil erosion; Glacial geology

Introduction

Soil geomorphology is a powerful tool that has been successfully used to correlate Quaternary deposits in a variety of environments (Birkeland, 1999). Pioneering work on glacial sequences in the North American Cordillera relied on the degree of soil development to estimate the ages of moraines (e.g., Richmond, 1965). The number and sophistication of investigations using soil development to correlate glacial deposits has increased dramatically in recent decades (e.g., Hall and Shroba, 1993, 1995). These correlations are possible because soils integrate the effects of weathering and erosion processes, which are fundamentally controlled by the climate, biota, topography, and age and composition of the soil parent materials (Jenny, 1941). The method requires that (1) soil-forming factors are effectively invariant among the different soils, (2) no major changes in soil-forming factors have occurred, and (3) a statistically significant relationship exists between selected soil properties and soil age. Soil sequences that fulfill these requirements are referred to as chronosequences.

The Quaternary geomorphology of southern Argentina is comprised of spectacular sequences of glacial moraines and associated outwash terraces (Clapperton, 1993). During ice ages, mountain glaciers expanded and coalesced to form the Patagonian Ice Cap. Outlet glaciers eroded deep valleys through the mountains and advanced out onto the flat plains east of the Andes at some locations. In the Lago Buenos Aires (LBA) valley, glaciers advanced as far as 100 km from the mountain front. Caldenius (1932) was the first to study the glacial deposits in Patagonia; he described four glacial advances and correlated them to the four-fold sequence in his native Scandinavia (three advances of the last glaciation, and one older advance). More recent studies at the Strait of Magellan (Clapperton et al., 1995), Lago Argentino (Mercer, 1976), and LBA (Singer et al., 2004), have confirmed Caldenius' mapping of deposits, but K–Ar and $^{40}Ar/^{39}Ar$ dating of basalt flows interbedded with glacial deposits indicates that the sediments are much older than

* Corresponding author.
E-mail address: douglass@geology.wisc.edu (D.C. Douglass).

0033-5894/$ - see front matter © 2005 University of Washington. All rights reserved.
doi:10.1016/j.yqres.2005.08.027

Caldenius' original interpretations, with the most extensive glacial advances occurring slightly over a million years ago (Mercer, 1976; Singer et al., 2004).

Three young basalt flows at LBA and almost 100 cosmogenic–nuclide surface-exposure ages (described below) yield one of the best-resolved long-term chronologies of glacial deposits in southern South America. However, the development of similar chronologies at other locations in Patagonia is hampered by the limited spatial distributions of lava flows. The two main goals of this study are to investigate the mechanisms and rates of soil formation and to identify soil properties that can be used to correlate other moraine sequences in Patagonia to this highly resolved chronology.

Physical setting

The soils investigated are situated on or near the crests of Quaternary moraines east of LBA (Fig. 1), about 50 km east of the Andean Cordillera. The mean annual air temperature is 9°C and the mean annual precipitation is 200 mm yr^{-1}, based on a decade of local climate observations and longer regional records.[1] Average summer (Dec.–Feb.) and winter (June–Aug.) temperatures are 14°C and 3°C, respectively. Approximately 75% of the annual precipitation falls between April and September (late fall through early spring). Summer winds are strong and persistently from the west; winter winds are weaker and more variable. The study area is part of the Southern Patagonian Steppe eco-region and contains semi-desert, shrub-steppe, and grass-steppe vegetation types (Soriano, 1983); the amount of bare ground varies from 40 to 70%.

Wind erosion, transportation and deposition are active processes in this windy, sparsely vegetated environment. The 1991 eruption of Volcán Hudson deposited about 10 cm of ash over most of this field area (Inbar et al., 1995). A decade later, most of this material has been removed. The only ash that remains is sand-sized grains in the lee of shrubs and boulders. It is not clear how much ash was incorporated into the soil and how much was removed from the field area by wind erosion. Fine-grained proglacial lake sediments exposed along the shores of LBA are also easily eroded during dry, windy conditions. These lake sediments are calcareous and are therefore a potential source for both carbonate and clay-sized particles. Dust from sedimentary rocks to the east could also be delivered to this field area by the easterly winds that occasionally occur in the winter.

The Quaternary drift of the LBA area first mapped by Caldenius (1932) was described as "one of the most complete and intact sequences of Quaternary moraines in the world" by Clapperton (1993; p. 358). Several workers have revisited the moraines (see Singer et al., 2004 for a summary of mapping efforts), and even though the resulting maps are all quite similar, the chronologic interpretations have been quite different. We adapt the chronology of Singer et al. (2004), who identified four moraine groups on the basis of moraine geomorphology and stratigraphic relationships to three $^{40}Ar/^{39}Ar$ dated basalt flows. The moraine groups are informally named, from youngest to oldest, the Fenix, Moreno, Deseado, and Telken moraines. The 109,000 ± 3000 yr (±2σ) Cerro Volcán flow separates the younger Fenix moraines from the older Moreno and Deseado moraines, and the 760,000 ± 14,000 yr (±2σ) Arroyo Page flow separates the younger Moreno and Deseado moraines from the older Telken moraines. The 1.016 ± 0.010 myr (±2σ) Arroyo Telken flow is the upper limit for the Telken moraines.

Refinement within this chronologic framework comes from ^{10}Be and ^{26}Al cosmogenic surface-exposure ages. Sixty-one analyses from 49 boulders on the five Fenix moraines and the Menucos moraine yielded ages between 22,700 and 14,400 yr (Kaplan et al., 2004; Douglass, 2005). Twenty-six analyses from 13 boulders on the two inner Moreno moraines yielded ages of approximately 140,000–150,000 yr, or marine oxygen isotope stage (MIS) 6; there are insufficient data to determine the age of the fragmented outer Moreno III moraine reliably (Kaplan et al., 2005). The ages of the Deseado moraines are poorly constrained. Stratigraphically, they are older than the Moreno moraines but younger than the Arroyo Page flow; they are therefore estimated to be between 200,000 and 760,000 yr old.

Despite their antiquity, the landforms in this environment are exceptionally well preserved. The Telken moraines are over 760,000 yr old and are subdued, but identifiable, landforms; braiding patterns are still preserved on outwash associated with these moraines. The slopes near the sampling sites averaged 5% on the youngest Fenix moraines and were less than 5% for older moraines. The mean elevations for soil sampling sites on the Fenix, Moreno, Deseado, and Telken moraines were 460 m, 520 m, 590 m, and 650 m, respectively.

The soils are formed in gravelly supraglacial sediment but sometimes extend into a more compact basal till. Glacier ice flowed about 150 km from the center of the Patagonian Ice Cap to the ice margins, eroding several different rock types, including rhyolites, granites, basalts, and other metamorphic and sedimentary rocks, including a marble unit (Lara et al., 2002; Servicio Geológico Nacional Argentino, 1994). The supraglacial sediment is typically a brown to pale brown (2.5Y 5/2; 10YR 4/2, 5/2), gravelly to very gravelly loamy sand that has a loose consistence. The basal till is similar to the supraglacial till but has lower gravel percentages and a much harder consistence. One important difference between the two types of parent materials is that the supraglacial sediments are generally carbonate-free, whereas the basal tills contain 1–4% calcium carbonate.

There have been few pedological studies in Patagonia. Several studies investigated eolian sedimentation in the Pampas north of Patagonia (Ramsperger et al., 1998; Zárate, 2003). Laya (1977) studied a vertical succession of Holocene ashes and the interbedded paleosols in Neuquén Province (Fig. 1). The soils were situated along a steep precipitation gradient and

[1] Temperature and precipitation data for Perito Moreno and several surrounding climate stations are taken from the United States National Center for Atmospheric Research dataset ds570.0 "World Monthly Surface Station Climatology, 1738-cont" available at http://dss.ucar.edu/datasets/ds570.0/.

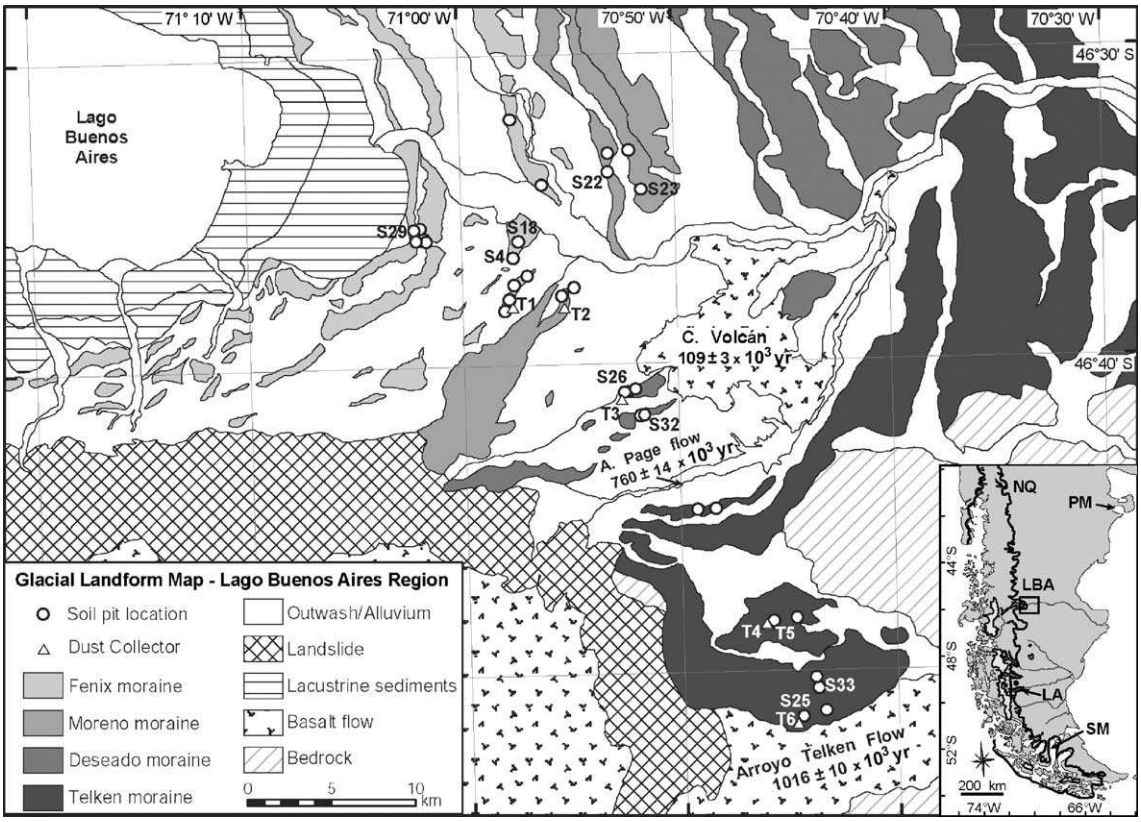

Figure 1. Geomorphology of the Lago Buenos Aires area and locations of soil sampling sites and dust collectors. Soil excavation numbers are preceded with S, dust collectors with T. Inset: Location map of southern South America and outline of detailed mapping. NQ—Neuquén, PM—Puerto Madryn, LBA—Lago Buenos Aires, LA—Lago Argentino, SM—Strait of Magellan.

showed increasing pH and cation-exchange capacity with decreasing moisture along this transect. Favier Dubois (2003) describes a buried soil seen in several archeological sites in southernmost Patagonia that dates to about 1000 ^{14}C yr B.P. These authors hypothesize that the burial of this soil is related to climate fluctuations related to the Medieval Warm Period. Scanning electron microscopy studies of soils near Puerto Madryn (300 km northeast of LBA) show the accumulation of "fine dendritic grains" of calcium carbonate that were interpreted to be of eolian origin and did not show signs of solution or recrystallization; opal spherules of unknown origin were also reported (Vogt and Larqué, 1998). A national soils map of Argentina depicts Aridisols and Mollisols in this region of Patagonia (INTA, 1990).

Methods

All pedons are situated on or near the crests of moraines in locations that appear to be stable and have representative vegetational cover and surface boulder frequency. Soils were excavated by hand and every effort was made to expose the full soil thickness, but this was not possible in all cases. Soils were described and sampled according to Schoeneberger et al. (2002). Percentages of coarse fragments were visually estimated in the exposed wall of the soil pit. Bulk samples were passed through a 2-mm sieve in the field. Fine-earth fractions were returned to the laboratory for characterization.

Bulk density was measured for nine of the 34 soil profiles using the compliant cavity procedure (method 4A5, Soil Survey Staff, 1996), correcting for >2 mm coarse-fragment content. Data from these profiles were used to generate an equation that was used to estimate bulk density for all of the soil horizons. Plotting measured bulk density against measured organic carbon concentration produced a statistically significant linear regression (n = 32, r^2 = 0.132, P = 0.04):

$$\text{Bulk density}\left(g\ cm^{-3}\right) = 1.85 - 0.28 \times \%\ \text{organic carbon} \quad (1)$$

The y axis intercept (1.85) is similar to the value expected for unconsolidated sediment with minimal excessive void spaces. The data used in this regression are presented in the data supplement (Table S-1).

Soil samples were sent to the University of Missouri Soil Characterization Laboratory, where analyses were performed using methods established by the Soil Survey Staff (1996), including particle-size distribution with sand fractionation (method 3A), pH and electrical conductivity in distilled water (8Cla and 8I, respectively), NH_4OAc-extractable bases (5B1), $BaCl_2$-triethanolamine-extractable acidity (6H1), cation-exchange capacity (CEC) by NH_4OAc at pH 8.2 (5A2), and base saturation from summation.

Field descriptions and laboratory pH values were used to determine soil Profile Development Indices (PDI) for all soils

Table 1
Soil profile descriptions of representative soils in the Lago Buenos Aires area

Horizon	Depth (cm)	Thickness (cm)	Boundary	Munsell Color		Texture	Structure		Consistence		Roots	Carb. Morph.	Rxn w/ 10% HCl	Coarse Frags (%)		
				Dry	Moist		Primary	Second	Dry	Wet				St	Co	Gr
Fenix I Moraine (~16,000 yr)																
LBA-S-29																
A	0–23	16–23	CW	10YR4/3	7.5YR3/2	VGS	1cgr	1vfgr	DS	SO/PO	2vf	0	nr	0	0	40
Bw	23–48	20–29	AW	10YR6/3	10YR4/2	GSL	M	2msbk	DSH	SS/PO	1vf,f	0	nr	0	0	25
Bk	48–61	9–14	AW	10YR7/1	10YR4/2	GLS	2msbk	1tnpl	DS, DSH	SO/PO	1vf	I–II	st	0	5	20
2C	61–79	–	–	10YR7/2	2.5Y5/2	SL	3tkpl	–	DSH	SO/PS	1vf	0	st	0	0	10
Fenix IV Moraine (~22,000 yr)																
LBA-S-04																
A	0–18	14–21	AW	10YR4/4	10YR3/3	GSL	1mgr	–	DS	SS/PS	2vf,1f	0	nr	0	10	30
Bw	18–53	30–46	AW	10YR5/3	10YR4/3	GSL	M	2csbk	DSH	SS/PS	1vf,f	0	nr	0	3	30
Bk	53–72	16–22	AW	10YR7/1	10YR4/2	GSL	2mabk	–	DSH	SS/PS	1vf	II	sl	0	3	30
BCk	72–105	30–40	AW	10YR6/2	10YR4/2	VGSL	2fabk	–	DS-DSH	SS/PS	1vf	I	sl	0	0	40
C	105–110	–	–	2.5Y6/2	10YR5/2	VGSL	M	2mabk	DSH	SS/PS	0	0–I	vsl	0	0	50
LBA-S-18																
A	0–23	22–28	AW	10YR4/2	10YR3/2	VGLS	1msbk	–	DS	SS/PO	2vf,f,1m	0	nr	0	5	35
Bw	23–40	10–18	AW	10YR5/3	10YR3/3	GSL	2msbk	2fsbk	DSH	SS/PS	1vf, f, m	0	nr	0	10	20
Bk	40–79	35–41	CW	10YR7/2	10YR5/2	VGL	2msbk	1fsbk	DSH	SS/P	1m	II	st	0	10	35
BCk	79–155	–	–	10YR6/2	10YR5/2	GSL	2msbk	1fsbk	DSH	SS/PS	0	I	sl	0	5	20
Moreno I Moraine (~140,000 yr)																
LBA-S-22																
A1	0–19	15–20	AW	10YR4/3	10YR3/2	GS	1msbk	–	DS	SS/PO	2vf,f	0	nr	0	5	20
A2	19–29	8–11	AW	10YR5/3	10YR4/2	VGSL	1msbk	–	DS	SS/PS	1vf,f	0	nr	0	5	55
Bk	29–65	51–62	AW	10YR7/2	10YR5/2	VGSL	2mabk	2fabk	DVH	SS/PO	1f	III	st	15	10	35
BCk	65–137	–	–	10YR7/2	10YR5/2	GLS	1fsbk	–	DSH	SS/PO	0	I–II	sl	15	10	30
Moreno II Moriaine (~150,000 yr)																
LBA-S-23																
A	0–23	21–25	CW	10YR4/3	10YR3/2	GS	1msbk	–	DS	SS/PO	2vf,f,1m	0	nr	5	10	25
Bk	23–46	15–25	AW	10YR7/1	10YR5/2	GSL	3mabk	2fabk	DH	SS/PO	1f, m	III	ve	5	15	30
BCk1	46–60	7–18	AW	10YR7/2	10YR5/1	VGSL	2msbk	1fsbk	DSH	SS/PS	1f	II	st	0	5	35
BCk2	60–75	10–20	AW	10YR7/1	10YR5/2	VGSL	2fabk	–	DVH	SS/PO	1f	III	ve	0	10	45
BCk3	75–125	–	–	10YR7/2	10YR5/2	VGSL	2msbk	–	DSH	SS/PS	1f	II	st	0	5	35

Deseado I Moraine (200,000–760,000 yr)															
LBA-S-26															
A1	0–36	33–38	AW	10YR3/3	10YR3/2	GLS	1mgr	–	DS	SS/PO	1vf,f	0	nr	0	3	30
A2	36–48	8–16	AW	10YR5/3	7.5YR3/2	GLS	1fsbk	–	DS	SS/PO	1vf	0	nr	0	0	20
Bk1	48–81	26–38	AW	7.5YR7/1	2.5Y5/2	GLS	2csbk	–	DSH	SS/PS	1vf	III	st	0	3	25
Bk2	81–89	7–10	AW	7.5YR7/1	10YR5/2	GSiL	3msbk	–	DH	SS/PS	0	IV–III	st	0	3	15
2C	89–100	–	–	10YR7/1	10YR5/2	GSL	2msbk	–	DH	SS/PS	0	0	nr	0	3	20
Deseado II Moraine (200,000–760,000 yr)															
LBA-S-32															
A	1–14	14–18	CW	10YR4/3	10YR3/3	VGLS	1cgr	–	DS	SO/PO	2vf,1f, m	0	nr	0	3	45
AB	14–58	25–42	AW	10YR5/3	10YR4/3	VGSL	2cgr	3fgr	DSH	SS/PO	2vf,1f	0	nr	0	3	50
Bk	58–81	33–52	AW	10YR7/2	10YR6/3	VGLS	2msbk	–	DSH	SS/PO	1vf	III	ve	0	0	55
BCk	81–125	26–30	AW	10YR6/2	10YR4/2	EGLS	osg-M	–	DLO-DH	SO/PO	1vf	I	st	0	0	60
C	125–130	–	–	10YR6/3	10YR4/2	VGLS	osg	–	DS	SO/PO	0	0	vs	0	0	45
Telken V Moraine (760,00–1,016,000 yr)															
LBA-S-33															
A	0–40	34–58	CW	10YR3/3	7.5YR3/2	VKSL	1mgr	–	DS	SS/PS	2vf	0	nr	0	40	30
Bk	40–60	17–22	AW	10YR8/1	10YR6/3	KSL	2vkpl	2msbk	DSH	SS/PS	1vf	III+	ve	0	25	20
BCk	60–102	38–45	CW	10YR6/2	2.5YR5/3	KL	3tkpl	2msbk	DSH	S/P	1vf	II–I	st	0	25	25
C	102–105	–	–	10YR6/3	10YR4.5/2	KL	2ctkpl	2cabk	DH	S/P	–	0	sl	0	25	20
Telken VI Moraine (760,00–1,016,000 yr)															
LBA-S-25															
A1	0–20	22–19	AW	7.5YR3/2	10YR3/2	VGSCL	2msbk	2mgr	DH	SS/P	1vf,f	0	nr	0	5	50
A2	20–33	10–13	AW	10YR4/3	10YR4/3	VGSC	2msbk	2mgr	DH	SS/P	1vf	0	nr	0	5	45
Bk	33–84	42–51	AW	2.5Y8/2	10YR5/3	VGSiL	2msbk	–	DH	SS/P	1vf	III	ve	0	5	45
BC	84–118	–	–	5Y6/4	10YR5/3	EGSL	2msbk	2fabk	DH	SS/PO	0	I	st	0	5	60

Notes. Boundary: AW = abrupt wavy, CW = clear wavy.
Texture: EG = extremely gravely, VG = very gravely, G = gravely, VK = very cobbly, K = cobbly, S = sand, LS = loamy sand, SL = sandy loam, L = loam, SiL = silt loam, SCL = sandy clay loam, SC = sandy clay.
Structure: 1 = weak, 2 = moderate, 3 = strong; vf = very fine, f = fine, m = medium, c = coarse, tk = thick, vk = very thick, gr = granular, sbk = sub-angular blocky, abk = angular blocky, pl = platy, osg = single grain, M = massive.
Consistence: DLO = loose, DS = soft, DSH = slightly hard, DH = hard, DVH = very hard, SO = non-sticky, SS = slightly sticky, S = sticky, PO = non-plastic, PS = slightly plastic, P = plastic.
Roots: 1 = few, 2 = common, 3 = many, vf = very fine, f = fine, m = medium, c = coarse.
Carbonate morphology: From Gile et al. (1966).
Reaction w/10% HCl: nr = no reaction, vsl = very slightly effervescent, sl = slightly effervescent, st = strongly effervescent, ve = violently effervescent.
Coarse Fragments: Stone = 60–25 cm, Cobble = 25–7.5 cm, Gravel = 7.5–2 mm.

Table 2
Soil characterization data of representative profiles

Horizon	Depth (cm)	Grain Size Distribution (%)										pH	EC (dS/m)	OC (%)	$CaCO_3$ (%)	Max. Gypsum (%)	Exchangable Ions (cmol (+) kg^{-1})								Base Saturation Sum (%)
		Total			Silt Fraction		Sand Fractions										Ca	Mg	Na	K	Sum Bases	Neut. Acid.	Sum Cations	CEC	
		Clay	Silt	Sand	F	C	VF	F	M	C	VC														
Fenix I Moraine (~16,000 yr)																									
LBA-S-29																									
A	0–23	3	11	86	5	6	14	26	14	17	16	6.66	0.30	0.7	0.0	0.1	5.1	1.2	0.1	0.5	6.8	1.9	8.7	9.0	78
Bw	23–48	4	24	72	12	13	17	23	10	11	10	7.05	0.30	0.4	0.0	0.1	7.4	1.6	0.2	0.1	9.3	1.3	10.6	9.8	87
Bk	48–61	4	18	78	9	8	13	24	13	15	14	7.98	0.36	0.3	5.3	0.1	31.6	1.6	0.4	0.1	33.6	0.0	33.6	6.6	100
2C	61–79	3	47	50	30	18	17	18	6	5	5	7.99	0.37	0.4	6.1	0.1	31.0	2.0	0.4	0.1	33.5	0.0	33.5	7.8	100
Fenix IV Moraine (~22,000 yr)																									
LBA-S-04																									
A	0–18	11	35	54	16	19	16	15	7	2	15	6.94	0.31	0.9	0.0	6.8	1.9	0.1	0.9	9.7	2.5	12.2	11.1	80	
Bw	18–53	9	31	60	19	13	15	14	7	11	12	7.02	0.28	0.6	0.0	0.1	6.3	1.6	0.1	0.6	8.6	2.8	11.4	10.1	75
Bk	53–72	6	37	57	22	15	17	15	7	9	9	8.15	0.33	0.2	3.6	0.1	25.2	2.0	0.2	0.3	27.8	0.0	27.8	7.6	100
BCk	72–105	4	32	64	17	15	19	15	7	12	13	8.65	0.47	0.1	1.5	0.1	12.8	2.4	1.0	0.3	16.5	0.0	16.5	6.0	100
C	105–110	5	34	62	19	15	15	15	8	13	12	8.58	0.70	0.1	1.1	0.1	11.9	2.4	1.7	0.4	16.4	0.0	16.4	5.8	100
LBA-S-18																									
A	0–23	4	10	87	4	6	18	26	16	16	10	6.45	0.25	0.5	0.0	0.1	4.0	1.2	0.1	0.7	6.0	2.0	8.0	6.8	75
Bw	23–40	7	17	76	9	8	14	28	15	13	8	7.06	0.29	0.4	0.0	0.1	6.5	2.0	0.1	0.4	9.1	3.5	12.6	9.5	72
Bk	40–79	9	39	52	28	12	9	10	6	11	14	8.31	0.36	0.3	12.4	0.1	35.9	3.2	0.2	0.1	39.4	0.0	39.4	7.3	100
BCk	79–155	3	47	51	25	22	15	11	6	9	10	8.35	0.31	0.1	2.1	0.1	18.8	1.6	0.2	0.1	20.7	0.0	20.7	4.8	100
Moreno I Moraine (~140,000 yr)																									
LBA-S-22																									
A1	0–19	2	6	91	3	3	20	34	14	12	11	7.20	0.34	0.7	0.0	0.1	5.3	0.8	0.0	0.8	6.9	0.6	7.5	7.9	92
A2	19–29	11	23	67	14	9	15	21	9	10	11	7.02	0.34	1.1	0.0	0.1	9.5	1.6	0.1	0.7	11.9	2.6	14.4	13.0	82
Bk	29–65	4	23	73	13	10	11	17	10	16	19	8.24	0.34	0.1	2.3	0.0	27.1	1.2	0.2	0.1	28.6	0.0	28.6	5.8	100
BCk	65–137	2	20	79	10	10	12	20	12	15	21	8.36	0.33	0.1	1.4	0.0	16.7	1.6	0.2	0.1	18.5	0.0	18.5	4.9	100
Moreno II Moraine (~150,000 yr)																									
LBA-S-23																									
A	0–22	2	7	91	4	4	28	31	10	10	13	6.84	0.31	0.7	0.0	0.1	6.0	1.2	0.1	0.4	7.7	0.9	8.6	7.8	89
Bw	22–32	9	24	67	13	11	12	13	8	14	21	6.83	0.30	0.6	0.0	0.1	28.8	1.6	0.2	0.0	30.6	0.0	30.6	6.2	100
Bk	32–67	1	30	69	13	17	17	20	9	11	12	8.01	0.38	0.1	2.1	0.0	19.3	1.2	0.2	0.0	20.7	0.0	20.7	5.3	100
BCk1	67–107	6	28	66	16	12	10	13	7	14	22	8.11	0.40	0.1	4.0	0.0	29.6	1.9	0.2	0.0	31.8	0.0	31.8	6.7	100
BCk2	107–145	5	42	53	29	13	6	6	4	11	27	8.45	0.33	0.1	8.7	0.1	36.9	6.3	0.7	0.0	43.9	0.0	43.9	9.2	100

Deseado I Moraine (200,000–760,000 yr)																								
LBA-S-26																								
A1	0–36	6	9	85	4	5	18	33	14	11	9	6.95	0.34	0.6	0.0	0.1	7.9	1.6	0.1	0.3	10.0	1.4	11.4	10.9	87
A2	36–48	6	10	83	6	4	9	27	21	16	10	7.24	0.35	0.3	0.0	0.1	8.7	1.9	0.1	0.2	11.0	1.3	12.2	11.0	90
Bk1	48–81	7	18	75	12	7	9	25	20	13	9	7.95	0.43	0.2	7.7	0.0	37.9	3.1	0.2	0.1	41.3	0.0	41.3	9.6	100
Bk2	81–89	9	36	55	23	13	11	12	6	11	15	8.16	0.43	0.2	4.8	0.0	34.2	4.3	0.3	0.1	38.9	0.0	38.9	13.5	100
2C	89–100	5	38	57	22	17	18	16	8	8	7	8.33	0.32	0.2	0.0	0.0	13.7	4.7	0.3	0.2	18.9	0.0	18.9	15.4	100
Deseado II Moraine (200,000–760,000 yr)																								
LBA-S-32																								
A	1–14	6	7	87	4	4	11	27	18	16	15	6.62	0.34	0.7	0.0	0.1	6.3	1.5	0.1	0.8	8.6	1.1	9.7	8.8	89
AB	14–58	13	13	74	10	3	3	7	10	27	27	6.96	0.39	0.5	0.0	0.1	12.5	2.4	0.2	0.2	15.2	2.6	17.8	15.9	86
Bk	58–81	10	18	72	12	6	7	10	9	22	24	7.87	0.44	0.5	18.4	0.1	43.3	4.4	0.3	0.1	48.2	0.0	48.2	10.5	100
BCk	81–125	5	11	84	8	3	3	7	9	29	36	8.10	0.34	0.2	1.9	0.0	17.2	3.2	0.2	0.1	20.7	0.0	20.7	7.4	100
C	125–130	9	9	82	7	2	3	8	12	28	31	8.03	0.33	0.0	0.8	0.0	11.7	3.7	0.2	0.2	15.8	0.7	16.4	9.3	96
Telken V Moraine (760,000–1,016,000 yr)																								
LBA-S-33																								
A	0–40	11	14	75	8	6	15	21	12	14	14	7.22	0.47	1.1	0.0	0.1	24.1	2.3	0.1	0.6	27.2	1.1	28.3	16.1	96
Bk	40–60	19	33	48	26	7	5	12	10	11	9	7.96	0.47	0.6	26.9	0.1	42.7	4.0	0.2	0.3	47.1	0.0	47.1	13.2	100
BCk	60–102	16	38	46	17	21	14	18	8	0	6	8.58	0.40	0.1	5.1	0.0	41.6	8.5	0.5	0.3	51.0	0.0	51.0	15.9	100
C	102–105	14	31	55	19	13	13	16	7	9	11	8.55	0.48	0.1	2.0	0.0	26.1	6.0	0.6	0.3	33.0	0.0	33.0	11.6	100
Telken VI Moraine (760,000–1,016,000 yr)																								
LBA-S-25																								
A1	0–20	26	13	61	7	6	14	21	10	8	9	6.79	0.57	1.7	0.0	0.2	21.2	5.2	0.1	1.1	27.6	4.3	31.9	29.6	86
A2	20–33	39	16	46	10	5	7	9	8	11	12	7.07	0.56	1.4	0.0	0.1	33.4	9.5	0.2	0.7	43.9	7.4	51.2	46.1	86
Bk	33–84	17	29	55	21	8	11	11	7	13	14	8.10	0.47	0.3	12.0	0.0	51.8	11.1	0.4	0.4	63.8	1.1	64.9	34.0	98
BC	84–118	6	20	74	12	8	11	13	9	18	24	8.10	0.42	0.1	6.3	0.0	45.8	12.3	0.6	0.3	58.9	0.7	59.6	30.4	99

Notes. 1 Grain Size Distributions use the USDA particle size classes.
Sand = 0.05–2.0 mm; VF = 0.05–0.1 mm, F = 0.1–0.25 mm, M = 0.25–0.5 mm, C = 0.5–1.0 mm, VC = 1.0–2.0 mm.
Silt = 0.002–0.05; F = 0.002–0.02 mm, C = 0.02–0.05 mm.
Clay < 0.002 mm.

(Harden, 1982). This semi-quantitative measurement uses several parameters to evaluate the degree of soil development. Each soil horizon was compared to the original properties of the parent material and was awarded points proportional to the changes that have occurred. This value was multiplied by the thickness of the horizon and all horizon values were summed for each soil profile. PDI values were calculated for the following parameters: rubification, color paling, melanization, color lightening, total texture, dry consistence, structure, pH, and carbonate morphology.

Total organic and inorganic carbon measurements were measured with a Leco CNS-2000 analyzer. Samples from each horizon were homogenized and pulverized to pass through a 100-mesh sieve. Two samples were analyzed for each horizon; an untreated sample was used to determine the total carbon content of the soil (i.e., organic carbon plus carbonate). The other sample was heated at 300°C in a muffle furnace for 24 h to combust organic material and was then used to determine the carbonate content of the soil. Organic carbon was calculated as the difference between total carbon and carbonate content. Combustion temperatures inside the LECO are ~1300°C, high enough to oxidize all forms of carbonate. Accordingly, we are unable to differentiate between calcite and other forms of carbonate, such as dolomite.

A-horizon quantities of organic carbon, and profile quantities of exchangeable cations, sum of exchangeable bases, and cation-exchange capacity were calculated following standard methods (Birkeland, 1999). For each horizon, the percent by mass of the constituent was multiplied by the bulk density and the thickness of the horizon, with a correction for the percentage of coarse fragments in the soil. The horizon values were summed to determine the profile quantity. Profile accumulation of clay-sized particles[2] and carbonate were calculated in a similar manner, except the percent by mass of the constituent in the parent material was subtracted from the horizon value to account for the original starting composition (Birkeland, 1999). For soils that did not penetrate the C-horizon, or for those soils that terminated at a lithologic discontinuity (e.g., till over lake sediments, or till over glaciofluvial sediments), an average composition derived from all similar parent materials was used as a proxy. Also, no assumptions were made about total soil thickness for partial soil descriptions; in these cases, profile quantities or accumulations are minimum values.

These horizon and profile quantities were regressed with four mathematical models to examine the relationship between pedogenic accumulation and soil age. The first three models are linear ($y = A + Bx$), log-linear ($y = A + lnB$), and power–law ($y = Ax^B$) regressions. These regressions are frequently used in soil chronosequence studies (Schaetzl et al., 1994) and require little explanation. The fourth model is a reservoir model that was originally developed to track changes in soil organic carbon (Jenny et al., 1949); it consists of a linear input function and a loss function that is dependent on the concentration of the constituent (i.e., a zero-order input function and first-order loss). In this model, the instantaneous accumulation rate is defined by:

$$\frac{dQ}{dt} = I - kQ \tag{2}$$

where I is the input function representing steady accumulation of the constituent and is independent of its concentration in the soil. The second term is the first-order loss function, where the rate of loss is proportional to a rate constant k and the quantity of the constituent in the soil Q. The time integral of this equation is:

$$Q = \frac{I}{k} \times \left(1 - e^{-kt}\right) \tag{3}$$

This equation produces curves that are similar to log-linear functions but have three distinct advantages for modeling some pedogenic processes. First, Eq. (3) necessarily passes through the origin, whereas logarithmic equations cannot. Logarithmic equations thereby fail to replicate the important boundary condition that pedogenic accumulation is zero at the initiation of soil development. Second, while logarithmic functions are commonly used to regress changes in soil properties with time, it is not clear that the mechanisms are governed by logarithmic mathematics. It can easily be argued that loss functions in soils should be proportional to concentration. If the loss is due to chemical leaching, higher concentrations of the constituent in the soil will increase the leaching potential of a given quantity of downward percolating water. Conversely, if the loss is due to erosion, higher concentrations will lead to greater losses at any given erosion rate. Finally, this regression equation leads to better correlation coefficients for most properties (see Results and interpretations).

Both long-term and interval-specific accumulation rates are calculated for carbonate and clay-sized particles. The long-term accumulation rate is defined as the total amount of accumulation divided by the age of the soil and yields an average rate of accumulation over time. The interval-specific accumulation is calculated by examining differences between sequential moraine groups in the chronosequence (Schlesinger, 1990). For example, the accumulated material in the Moreno soils minus that in the Fenix soils represents the accumulation that occurred between ~140,000 and ~20,000 yr ago. The rate is determined by dividing this accumulation by the duration of this time interval. Variability of accumulation within each moraine group is propagated through this analysis. This analysis assumes that the accumulation rate of the constituent in the soil is constant across the entire field area at any given moment.

To measure dust composition and deposition rate across this field area, six dust collectors were installed in a transect downwind from these lake sediments (locations shown in Fig. 1). We used plastic dishpans measuring 35 by 30 cm and 11 cm deep, filled with 2.5 cm of marbles. They were positioned 50–75 cm above the ground surface on rock cairns to reduce the collection of local saltating load. Products such as Tanglefoot® were not used to prevent animal activity in and around the dust

[2] In this paper, the term clay refers to clay-sized particles and not to mineralogy.

collectors as suggested by Reheis and Kihl (1995). However, there was no evidence of bird feces in the traps.

Analysis of Variance (ANOVA) and Fisher's test were used to test the statistical significance of trends in these data and were performed with the MINITAB software package. Linear and log-linear regressions were calculated in Excel by standard least squares methods. Nonlinear least squares regressions were performed with the S-Plus software package. The Gauss–Newton algorithm was used with a matrix of bracketing initial values to ensure convergence on the best values. Correlation coefficients (r^2) were determined as the ratio of regression sum of squares to total sum of squares.

Results

Soil morphology and characterization

Profile descriptions, and soil-characterization and analytical data for nine representative soils from the four moraine groups are given in Tables 1 and 2, respectively; descriptions of all 34 soil profiles are given in the data supplement (Tables S-2). Most soils have a mollic epipedon over a calcic diagnostic horizon and generally are classified as coarse-loamy, mesic, Typic Calcixerolls or Calcic Haploxerolls (Soil Survey Staff, 1999; Table 1; data supplement). Soil textures are generally either gravelly sandy loam or gravelly loamy sand (Table 1). Total sand percentages commonly decrease with soil depth; surface horizons typically have more fine sand (0.10–0.25 mm), and subsurface horizons have greater percentages of coarse sand (0.5–1.0 mm) (Table 2). Soil pH, electrical conductivity, exchangeable bases (especially calcium), and base saturation increase with depth in most soil profiles (Table 2).

A-horizons typically have weak granular or sub-angular blocky structure, and they lack the vesicular porosity commonly observed in other arid and semi-arid soils (e.g., Gile and Grossman, 1979; McFadden et al., 1998). The soils near LBA have coarser textures than these other arid soils, typically loamy sand as opposed to loam textures, which lead to lower cohesion, weaker soil structures, and the instability of vesicular pores in these surface horizons. The organic carbon concentration of these surface horizons is typically ~0.7% by mass,

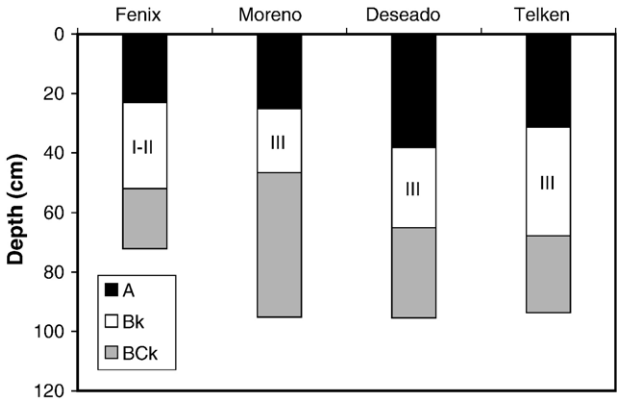

Figure 2. Average soil horizon thicknesses and carbonate morphology for the four moraine groups. Carbonate morphology from Gile et al. (1966).

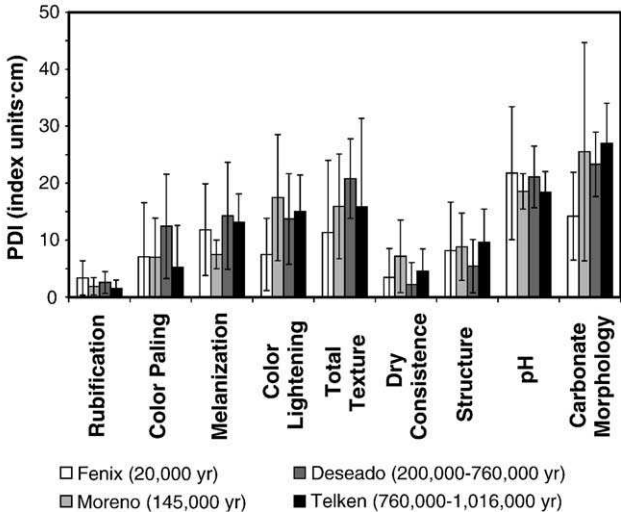

Figure 3. Profile-development index parameters for the four moraine groups. Error bars represent one standard deviation. The only statistically significant differences between different moraine groups is for the color lightening parameter between the Fenix and Moreno groups ($P = 0.03$).

but it is higher for the oldest Telken soils, which have ~1.3% organic carbon (Table 2 and data supplement). Some of the older soils have an A2 or AB-horizon, which have slightly higher silt and clay contents than the surface A-horizon, but do not show signs of clay translocation (e.g., clay skins). The thickness of the A-horizons generally increases with soil age (Fig. 2), but differences between moraine groups are not statistically significant.

The carbonate in the calcic horizons is a mixture of fine powdery carbonate in the matrix and laminar rinds that have precipitated on coarse clasts. Petrocalcic horizons are not present in any of the soils on moraines, but they are sometimes seen in the Telken outwash soils. The thicknesses of the Bk and BCk-horizons generally increase with soil age (Fig. 2), but as with A-horizon thicknesses, these differences are not statistically significant. There is a significant increase in average carbonate morphology from I–II to III between the Fenix and Moreno soils; however, carbonate morphology plateaus and remains at III for the Deseado and Telken soils. Carbonate concentrations in the calcic horizons show the same trends as carbonate morphology; Fenix Bk-horizons have ~5% carbonate, whereas the Moreno, Deseado, and Telken Bk-horizons all have ~15% carbonate.

Gypsum is a common feature in many arid soils (e.g., Eswaran and Zi-Tong, 1991) but is not present in these soils. Analysis of several samples of gypsum standard in the Leco CNS-2000 showed that concentrations of gypsum could be accurately determined with the sulfur component of this analysis. No horizon has a calculated gypsum concentration higher than 0.3%. For B-horizons, where gypsum is expected to reside, calculated concentrations are always less than 0.1% (Table 2). There is a strong positive correlation between sulfur and organic carbon concentrations suggesting that most of the sulfur is derived from organic matter.

Pedogenic silica is also commonly found in arid and semi-arid soils (e.g., Boettinger and Southard, 1991; Harden et al.,

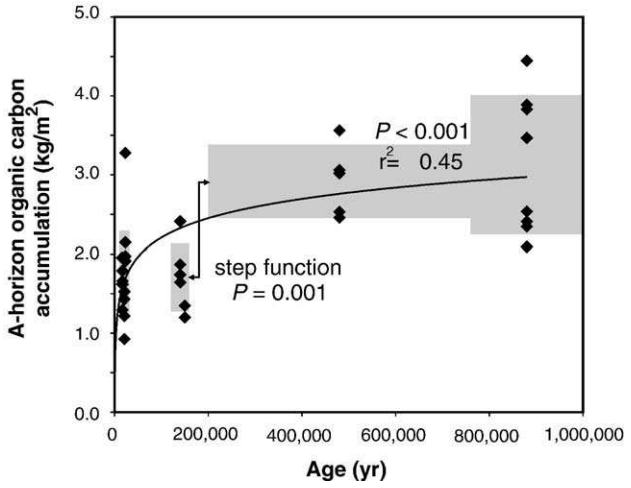

Figure 4. Quantity of organic C in the A-horizon plotted against soil age. Vertical dimension of gray boxes represent one standard deviation within each moraine group; horizontal dimension represents uncertainty in moraine age. See text for interpretations of step function and log-linear regression.

1991), but it is not present in sufficient amounts to cement soils of the LBA area. Peds from the hard, dense horizons did not slake any faster in concentrated NaOH than in water (a diagnostic field test for duricrete: Soil Survey Staff, 1999). Vogt and Larqué (1998) report nanometer-scale filaments and spherules of pedogenic silica in northern Patagonian soils based on scanning electron microscopy, but there was no attempt to determine profile quantities of pedogenic silica in that study.

Profile development indices

Profile Development Indices (PDI; Fig. 3; Data supplement Table S-3) corroborate morphologic observations. Color lightening, total texture and carbonate morphology generally increase with soil age; however, the only statistically significant difference in PDI values is for the color lightening parameter between the Fenix and Moreno soils (P = 0.03). While the increases in the total texture and carbonate

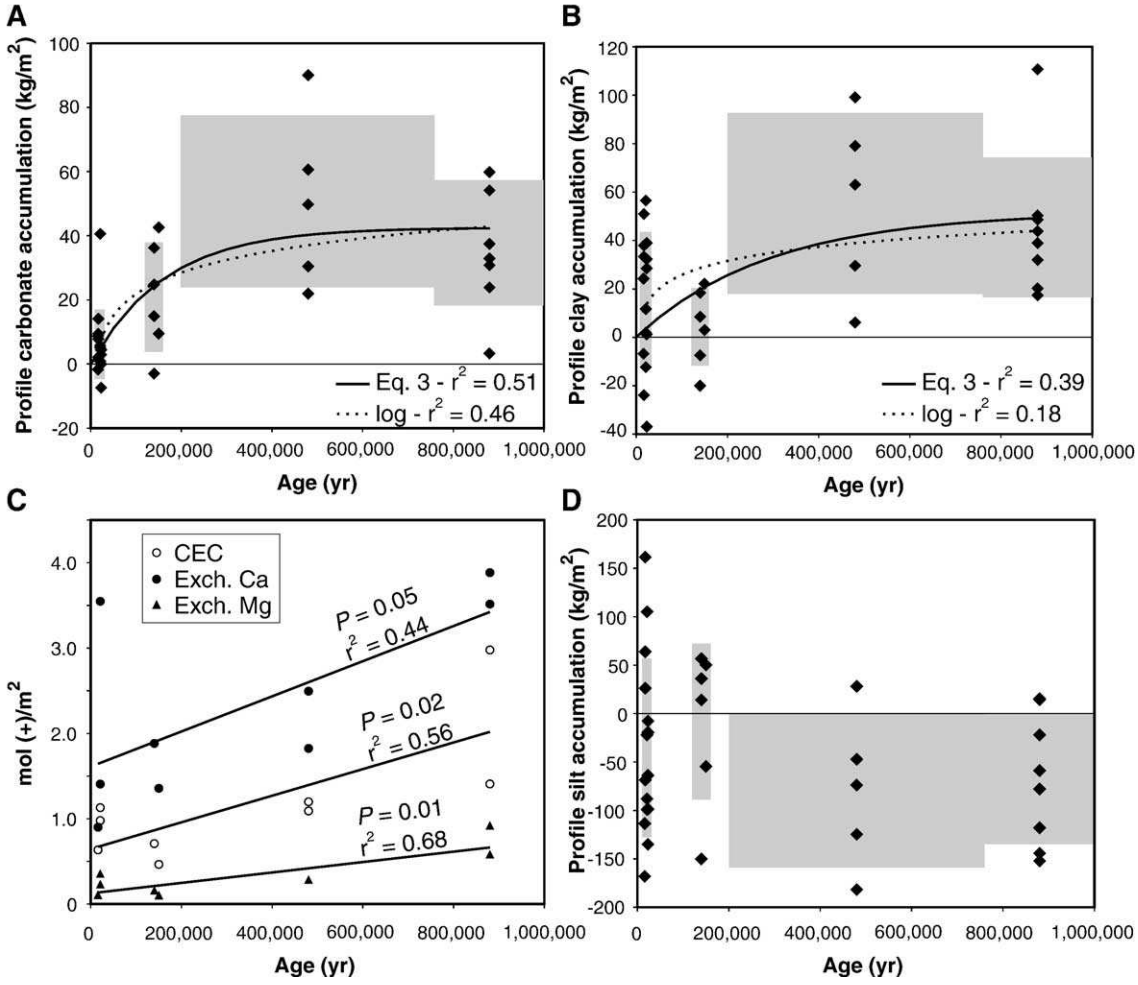

Figure 5. Accumulation (or loss) of pedogenic products in soils. (A) Accumulation of pedogenic carbonate, (B) accumulation of clay-sized material, (C) profile quantities of exchangeable bases, and (D) loss of silt from soils. Vertical dimension of gray boxes represent one standard deviation within each moraine group; horizontal dimension represents uncertainty in moraine age.

morphology PDI parameters are not statistically significant, there are significant age-related increases in profile accumulations of clay and carbonate (see below). Also, the static melanization PDI parameter failed to describe the statistically significant increases in A-horizon quantities of organic carbon with soil age (described below). There were no appreciable differences among moraine groups in the rubification, color paling, dry consistence, structure, and pH PDI parameters.

Horizon or profile quantities of pedogenic products

A-horizon quantities of organic carbon range between about 1 and 4 kg m^{-2} and are highest for the Deseado and Telken soils (Fig. 4). On average, the Deseado soils have thicker A-horizons (Fig. 2) and Telken soils have higher organic carbon concentrations (Table 2). These data can be described as a highly significant ($P = 0.001$) step function increase between the Moreno and Deseado soils, with similar horizon quantities for the Fenix and Moreno as well as the Deseado and Telken soils. However, these trends also fit a log-linear regression ($r^2 = 0.45$; $P < 0.001$), which would require that soil organic matter is exceedingly stable in this environment (see Discussion).

Profile accumulations of pedogenic carbonate and clay-sized particles are also significantly correlated with time (Figs. 5A, B) and are best fit with Eq. (3) ($r^2 = 0.51$ and 0.38, both $P < 0.001$). These data can also be fit with log-linear regressions, but these regressions have lower correlation coefficients ($r^2 = 0.46$ and 0.18 or $P < 0.001$ and 0.01, for carbonate and clay, respectively), and as explained in the methods section, it is not clear that mechanisms of soil formation are governed by logarithmic mathematical functions. The best-fit parameters for carbonate indicate accumulation at 0.26 g m^{-2} yr^{-1}, with a rate constant (1/k) of 163,000 yr and an equilibrium profile quantity of ~43 kg m^{-2}. The rate of clay accumulation is slightly lower, 0.18 g m^{-2} yr^{-1}, but it approaches equilibrium more slowly (1/k = 293,000 yr). The equilibrium profile quantity of clay is ~52 kg m^{-2}. The mechanisms responsible for the decreased accumulation rates in the older soils are discussed below.

Exchangeable Ca, Mg, and cation-exchange capacity also show significant positive correlation with time, but in contrast to the accumulations of carbonate and clay, these parameters are best fit with linear regressions (Fig. 5C; $r^2 = 0.44$, 0.68, and 0.56, respectively, corresponding to $P = 0.05$, 0.02, and 0.01). The sum of base cations also shows significant positive correlation with age, but this parameter is not graphed because it is dominated by Ca and therefore demonstrates similar trends. In contrast, silt generally declines in the profiles over time; however, these trends are not statistically significant (Fig. 5D).

Dust composition and deposition rate

Only one of the six dust collectors remained completely undisturbed after 1 year of deployment, from which we calculate a dust deposition rate of 27 g m^{-2} yr^{-1} and a carbonate deposition rate of 1.2 g m^{-2} yr^{-1}. Three other collectors remained upright and collected similar amounts of material, but each had shifted enough that the collected dust was only analyzed for composition, not rate of deposition (Table 3). Three of the four samples have ~4% organic carbon and ~5% carbonate. The fourth sample has lower organic carbon and carbonate concentrations (both ~1.5%) and greater amounts of sand (based on visual observation and hand texturing). This collector was closest to the ground, and we infer it collected more local saltating load than the other collectors. These rates of dust deposition are comparable to arid and semi-arid environments in the southwestern United States (Reheis et al., 1995) and the Argentine Pampas (Ramsperger et al., 1998).

Table 3
Dust deposition rate and composition

Collector	Location	Deposition Rate (g m^{-2} yr^{-1})	Organic Carbon (%)	Carbonate (%)
1	Fenix	–	–	–
2	Moreno	–	3.7	4.9
3	Deseado	–	1.6	1.4
4	Telken	27.1	3.4	4.4
5	Telken	–	–	–
6	Telken	–	5.9	5.4
Average composition =			3.7	4.0

Discussion

Mechanisms and rates of soil formation

The three most important soil-forming processes in these soils are melanization, calcification, and the accumulation of clay-sized particles. It is clear that most of the organic carbon has accumulated in these soils quite quickly, i.e., in the last ~15,000 yr, but we cannot rule out the possibility that organic carbon may continue to accumulate over much longer periods of time. Continually increasing quantities of organic carbon over hundreds of thousands of years requires that organic carbon is exceedingly stable in this environment; however, most studies suggest that soil organic carbon equilibrates in less than 5000 to 20,000 yr, even in arid environments (Birkeland, 1999, and references therein). Based on this prior work, our preferred interpretation is that the greater accumulation of organic carbon in the Deseado and Telken soils is not related to soil age but to slight differences in soil environment such as microclimate effects, moisture retention, or grazing practices. The older soils are at higher elevations, leading to increased effective precipitation due to greater winter snowfall and decreased summer temperatures, but they also have finer soil textures, which leads to increased moisture retention or increased soil fertility. Sheep have also grazed this region for the last 80–100 yr. Different grazing practices on each ranch, and the resulting soil degradation, may account for some of this variability.

Accumulation rates of carbonate and clay-sized particles are lowest for the Telken soils, which are both oldest and furthest away from the lake sediments, one of the more mobile dust sources. To investigate the role of transport distance, the long-term rates of accumulation are plotted against distance from the lake sediments (Figs. 6A, B). These data can be fit with weak,

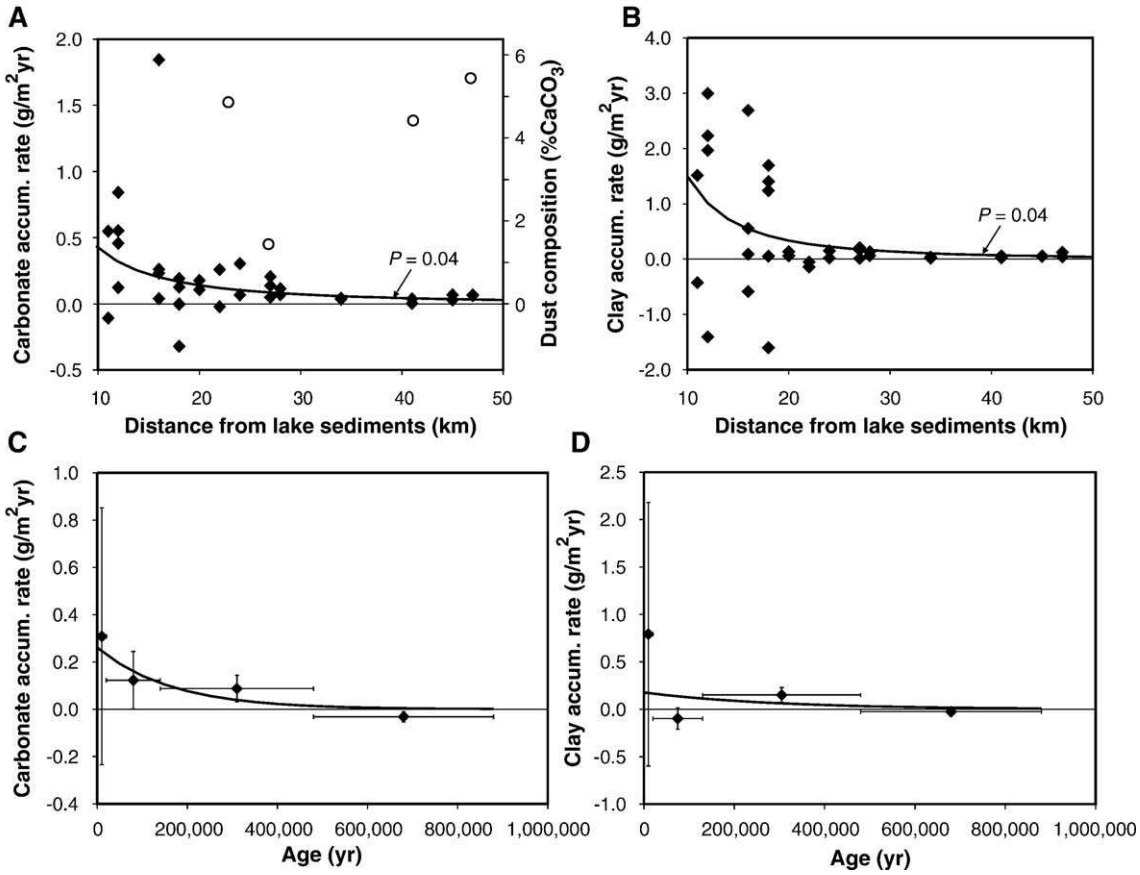

Figure 6. Long-term and interval-specific accumulation rates of carbonate and clay-sized material. (A) Long-term carbonate accumulation rate plotted against distance from lake sediments (solid diamonds) fit with a power–law regression ($P = 0.04$), and modern carbonate concentration in dust samples (open circles). (B) Long-term accumulation of clay-sized particles plotted against distance from lake sediments fit with a power–law regression ($P = 0.04$). (C) Interval-specific (points with error bars) and best-fit long-term (line) carbonate accumulation rates. (D) Interval-specific (points with error bars) and best-fit long-term (line) accumulation rates of clay-sized particles.

but statistically significant ($P = 0.04$) power–law regression, which suggests that accumulation rates decrease downwind from the lake sediments. However, this interpretation is at odds with the four measurements of dust composition (Table 3; open circles in Fig. 6A). Three of the four samples indicate that the carbonate concentration of the dust deposited across the field area appears to be relatively uniform, with the fourth anomalous sample interpreted to contain reduced amounts of carbonate and organic carbon because of dilution by greater amounts of locally derived saltating sand. This suggests that transport distance may not be an important factor in the decreased accumulation rates on these distal soils. We recognize that these are concentration, not flux measurements, and that more data are needed to test this relationship fully.

Both the long-term and interval-specific carbonate and clay accumulation rates show decreased rates for the older soils (Figs. 6C, D). Similar plateaus are seen in many other soil chronosequence studies, although the time required to reach equilibrium depends on the constituent and the environment (Bockheim, 1980; Birkeland, 1999). Following other workers, we present two working hypotheses: (1) accumulation rates were lower in the earliest part of the record, or (2) some process acts to limit accumulation in these soils, perhaps by slow or episodic soil erosion (e.g., Nikiforoff, 1949; Johnson and Watson-Stegner, 1997). Unfortunately, this first hypothesis is effectively untestable because reliable reconstructions of influx rates is only possible if there are no losses from the soil, or if the losses are quantifiable.

In the second hypothesis, erosion removes clay and carbonate from the soils, either slowly or episodically, and is supported by the lack of petrocalcic horizons in these soils. Glacial climates may have led to decreased vegetation cover and increased wind speeds, facilitating the stripping of the surface of the soil until a desert pavement could form. If cryoturbation was an active process in these soils, then this could continually prevent the development of a protective pavement, continually bringing clay and carbonate to the surface (e.g., Bruce, 1973; Hall, 1999). A second mechanism of loss could be related to burrowing animals such as dwarf armadillos (*Zaedyus pichiy*), which bring fine materials to the surface that are then carried away by the wind (e.g., Burns, 1979). Finally, simple down-slope movement of surface material may be sufficient to explain the loss of clay and carbonate from these soils. The erosion hypothesis is supported by the subdued morphology of the older moraines, but rates must have been slow, otherwise the very old moraines would

not be preserved. The cosmogenic surface-exposure data from this field area also support limited landscape modification in this area. Seven of 49 boulders (14%) from the Fenix moraines have anomalously young ages and are interpreted to have been exhumed after moraine deposition (Douglass, 2005), although this exhumation may be the result of frost heave rather than erosion of overlying material.

Finally, there were no significant changes in soil redness (rubification PDI parameter), suggesting that oxidation of iron-bearing minerals is not a major soil-forming process in this environment. The zero-order rate of clay accumulation (0.18 g m^{-2} yr^{-1}), as determined from the regression of clay accumulation versus time, is more than two orders of magnitude less than the short-term rate of dust deposition in this area (27 g m^{-2} yr^{-1}). If the measured dust influx is representative of longer-term rates, then dust influx can explain all of the clay accumulation in these soils, even if the dust is only 1% clay. It is not clear how representative this single dust influx measurement is of the long-term average. The vegetation is still recovering from the eruption of Volcán Hudson, and many parts of Patagonia have been heavily impacted by intensive grazing. Nevertheless, it appears that much of the carbonate is derived from eolian dust and not from chemical weathering in these soils. Weathering rates are likely limited because of the dominance of winter precipitation, which allows some of the winter snowfall to sublimate back into the atmosphere before it can enter the soil. Also, temperatures are cold when the soils are moist, further limiting chemical reaction rates. Moreover, summer precipitation is often ineffective in soil formation because it is rapidly evaporated by the nearly constant winds.

Carbonate cycle

In our working model of the carbonate cycle in this environment (Fig. 7), pedogenic carbonate is derived from three sources: (1) carbonate cement contained within the Tertiary Santa Cruz Formation under the Quaternary sediments contained in this valley, (2) a marble unit in the Andean Cordillera 125 km to the west, and (3) pedogenic carbonate in the Tertiary Patagonian Gravel to the north and east of these moraines. Glacial erosion of the marble and the Santa Cruz Formation produces basal till units that contain 1–4% primary carbonate, which can be redistributed in the soil profile by pedogenic processes. The deposition of carbonate-enriched eolian dust derived from lacustrine deposits along the shores of LBA is another potentially important source of carbonate for these soils. These sediments were deposited in a proglacial lake that formed during deglaciation when the modern outlet at the west end of the lake was dammed by ice. This lake basin trapped large volumes of sediments, some of which were glacially eroded from the marble and the Santa Cruz Formation, and some of which were brought to the lake from the Patagonian Gravel by fluvial processes. These fine-grained sediments are easily eroded from unvegetated exposures by the strong and persistent winds in this area. It is also possible that carbonate dust is derived directly from the rock exposures themselves, but probably at a lower rate.

Elements of this model may only be applicable to the modern landscape, but similar proglacial lakes probably formed during the penultimate, and perhaps earlier, deglaciations. The absence of similar lacustrine sediments from much earlier landscapes (i.e., before glacial erosion had created the LBA overdeepening) may explain the apparently lower carbonate and clay accumulation rates in the earliest part of the record.

Correlation of glacial deposits in Patagonia

One of the objectives of this project is to develop correlation tools so that other glacial deposits in similar semi-arid settings of southern Patagonia could be quickly and easily compared to the well-dated Lago Buenos Aires moraines. The degree of soil formation on deposits is one way to make these correlations, provided the mechanisms and rates of soil formation are similar between the two locations. In each new field area, some constraint on either deposit age or rates of soil formation will be needed to test this assumption. Profile accumulations of carbonate, clay, and exchangeable bases appear to be the most useful soil parameters to examine, although it may be difficult to differentiate very old deposits with these methods. The field-based PDI method does not appear to work well in this environment; however, the measurement of carbonate concentration is a simple and reproducible measurement to make in the laboratory.

Conclusions

The dominant mechanisms of soil formation in this environment are melanization, calcification, and the accumulation of clay-sized particles. Soil organic carbon appears to equilibrate quickly but may continue to accumulate over very long periods

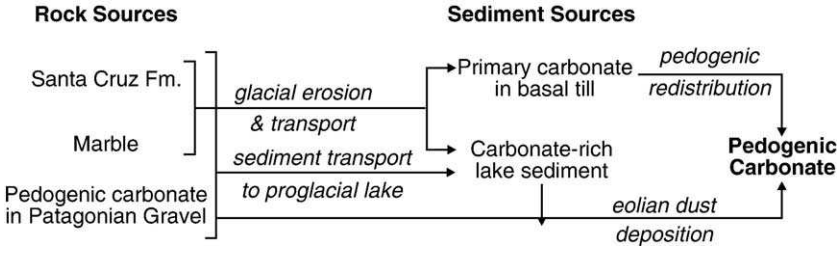

Figure 7. Preliminary descriptive model of the sources and processes leading to the accumulation of carbonate in the Lago Buenos Aires soils.

of time. Both long-term and interval-specific rates of carbonate and clay accumulation are highest on the younger soils and decrease with increasing soil age and distance from lake sediments near Lago Buenos Aires. However, because concentrations of carbonate in dust samples do not vary systematically across the field area, we propose that the decreased accumulation rates in the older soils are not a function of transport distance from the lake sediments. We find it more likely that these plateaus are the result of either lower influx rates during the early part of the record, or slow soil erosion limiting the accumulation of carbonate and clay-sized particles in these soils. More data are needed to evaluate these hypotheses.

Acknowledgments

This project was supported by the National Science Foundation Earth System History grant ATM-0212450. We appreciate the field and laboratory assistance of A. Frank, D. Mickelson, M. Gorring, M. Kaplan, S. McGee, and B. Singer. We thank J. Burt for assistance with the nonlinear regressions, as well as D. Hammer and R. Dresbach at the University of Missouri Soil Characterization Laboratory for their excellent work. We are grateful for the logistic support and friendship of Reynaldo (Coco) and Joan (Petti) Nauta of Estancia Telken, and the cooperation of all of the landowners in the Perito Moreno area.

Appendix A. Supplementary data

Supplementary data associated with this article can be found in the online version at doi:10.1016/j.yqres.2005.08.027.

References

Birkeland, P.W., 1999. Soils and Geomorphology, 3rd ed. Oxford Univ. Press, New York. (430 pp.).

Bockheim, J.G., 1980. Solution and use of chronofunctions in studying soil development. Gederma 24, 71–85.

Boettinger, J.L., Southard, R.J., 1991. Silica and carbonate sources for Aridisols on a granitic pediment, Western Mojave Desert. Soil Science Society of America Journal 55, 1057–1067.

Bruce, J.G., 1973. Loessial deposits of the South Island, with a definition of the Stewarts Claim Formation. New Zealand Journal of Geology and Geophysics 16, 533–548.

Burns, S.F., 1979. The northern pocket gopher (*Thomomys talpoides*): a major geomorphic agent in the alpine tundra. Journal of Colorado-Wyoming Academy of Science 11, 86.

Caldenius, C.G., 1932. Las glaciaciones Cuaternarias en la Patagonia and Tierra del Fuego. Geografiska Annaler 14, 1–164.

Clapperton, C.M., 1993. Quaternary Geology and Geomorphology of South America. Elsevier, Amsterdam. (779 pp.).

Clapperton, C.M., Sugden, D.E., Kaufman, D.S., McCulloch, R.D., 1995. The last glaciation in the central Magellan Strait, southernmost Chile. Quaternary Research 44, 133–148.

Douglass, D.C., 2005. Glacial Chronology, Soil Development, and Paleoclimate Reconstructions for Mid-Latitude South America, 1Ma to Recent. PhD Dissertation, University of Wisconsin-Madison. (212 pp.).

Eswaran, H., Zi-Tong, G., 1991. Properties, genesis, classification, and distribution of soils with gypsum. In: Nettleton, W.D. (Ed.), Occurrence, Characteristics, and Genesis of Carbonate, Gypsum, and Silica Accumulations in Soils, Soil Science Society of America Special Publication, vol. 26. Soil Science Society of America, Madison, WI, USA, pp. 89–119.

Favier Dubois, C.M., 2003. Late Holocene climate fluctuations and soil genesis in southern Patagonia: effects on the archaeological record. Journal of Archaeological Science 30, 1657–1664.

Gile, L.H., Grossman, R.B., 1979. The Desert Project Soil Monograph: Soils and Landscape of a Desert Region Astride the Rio Grande Valley, New Mexico. United States Department of Agriculture, Soil Conservation Service, U.S. Government Printing Office, Washington, DC. (984 pp.).

Gile, L.H., Peterson, F.F., Grossman, R.B., 1966. Morphological and genetic sequences of carbonate accumulation in desert soils. Soil Science 101, 347–360.

Hall, R.D., 1999. Effects of climate change on soils in glacial deposits, Wind River Basin, Wyoming. Quaternary Research 51, 248–261.

Hall, R.D., Shroba, R.R., 1993. Soils developed in the glacial deposits of the type area of the Pinedale and Bull Lake glaciations, Wind River Range, Wyoming. Arctic and Alpine Research 25, 368–373.

Hall, R.D., Shroba, R.R., 1995. Soil evidence for a glaciation intermediate between the Bull Lake and Pinedale glaciations at Fremont Lake, Wind River Range, Wyoming, U.S.A. Arctic and Alpine Research 27, 89–98.

Harden, J.W., 1982. A quantitative index of soil development from field descriptions: examples from a chronosequence in central California. Geoderma 28, 1–28.

Harden, J.W., Taylor, E.M., Reheis, M.C., McFadden, L.D., 1991. Calcic, gypsic, and siliceous soil chronosequences in arid and semiarid environments. In: Nettleton, W.D. (Ed.), Occurrence, characteristics, and genesis of carbonate, gypsum, and silica accumulations in soils, Soil Science Society of America Special Publication, vol. 26. Soil Science Society of America, Madison, WI, USA, pp. 1–16.

Inbar, M., Ostera, H.A., Parica, C.A., Remesal, M.B., Salani, F.M., 1995. Environmental assessment of 1991 Hudson volcano eruption ashfall effects on southern Patagonia region, Argentina. Environmental Geology 25, 119–125.

INTA, 1990, *Atlas de Suelos de la República Argentina*. Proyecto PNUD Arg-85/019, Buenos Aires. Dos tomos, 1600.

Jenny, H., 1941. Factors of Soil Formation. McGraw-Hill, New York. (241 pp.).

Jenny, H., Gessel, S.P., Bingham, F.T., 1949. Comparative study of decomposition rates of organic matter in temperate and tropical regions. Soil Science 68, 419–432.

Johnson, D.L., Watson-Stegner, D., 1997. Evolution model of pedogenesis. Soil Science 143, 349–366.

Kaplan, M.R., Ackert Jr., R.P., Singer, B.S., Douglass, D.C., Kurz, M.D., 2004. Cosmogenic nuclide chronology of millennial-scale glacial advances during O-isotope stage 2 in Patagonia. Geological Society of America Bulletin 116, 308–321.

Kaplan, M.R., Douglass, D.C., Singer, B.S., Ackert Jr., R.P., Caffee, M.W., 2005. Cosmogenic nuclide chronology of pre-last glaciation maximum moraines at Lago Buenos Aires, 46°S, Argentina. Quaternary Research 63, 301–315.

Lara, L., Cornejo, P., Suárez, M., Godoy, E., Arévalo C., 2002. Mapa geológico de Chile escala 1:1,000,000. Servicio Nacional de Geología y Minería Santiago, Chile.

Laya, H.A., 1977. Edafogenesis y paleosuelos de la formation tefrica Rio Pireco (Holoceno) suroeste de la Provincia del Neuquén, Argentina. Revista de la Asociatión Geológica Argentina 32, 3–23.

McFadden, L.D., McDonald, E.V., Wells, S.G., Anderson, K., Quade, J., Forman, S.L., 1998. The vesicular layer and carbonate collars of desert soils and pavements: formation, age and relation to climate change. Geomorphology 24, 101–145.

Mercer, J.H., 1976. Glacial history of southernmost South America. Quaternary Research 6, 125–166.

Nikiforoff, C.C., 1949. Weathering and soil evolution. Soil Science 67, 219–230.

Ramsperger, B., Peinemann, N., Stahr, K., 1998. Deposition rates and characteristics of aeolian dust in the semi-arid and sub-humid regions of the Argentinian Pampa. Journal of Arid Environments 39, 467–476.

Reheis, M.C., Kihl, R., 1995. Dust Deposition in southern Nevada and California, 1984–1989: relations to climate, source area, and source lithology. Journal of Geophysical Research D100, 8893–8918.

Reheis, M.C., Goodmacher, J.C., Harden, J.W., McFadden, L.D., Rockwell, T.K., Shroba, R.R., Sowers, J.M., Taylor, E.M., 1995. Quaternary soils and dust deposition in southern Nevada and California. Geological Society of America Bulletin 107, 1003–1022.

Richmond, G.M., 1965. Glaciation of the Rocky Mountains. In: Wright, H.E., Frey, D.G. (Eds.), The Quaternary of the United States. Princeton Univ. Press, Princeton, NJ, pp. 217–230.

Schaetzl, R.J., Barrett, L.R., Winkler, J.A., 1994. Choosing models for soil choronofunctions and fitting them to data. European Journal of Soil Science 45, 219–232.

Schlesinger, W.H., 1990. Evidence from chronosequence studies for a low carbon-storage potential of soils. Nature 348, 232–234.

Schoeneberger, P.J., Wysocki, D.A., Benham, E.C., Broderson, W.D., 2002. Field Book for Describing and Sampling Soils. National Soil Survey Center, Natural Resources Conservation Service, U.S. Department of Agriculture, Lincoln, NE.

Servicio Geológico Nacional Argentino, 1994. Mapa geológico de la Provincia de Santa Cruz, República Argentina. 1:750,000. Servicio Geológico Nacional Argentino, Buenos Aires, Argentina.

Singer, B.S., Ackert Jr., R.P., Guillou, H., 2004. $^{40}Ar/^{39}Ar$ and K–Ar chronology of Pleistocene glaciations in Patagonia. Geological Sociedty of America Bulletin 116, 434–450.

Soil Survey Staff, 1996. *Soil Survey Laboratory Methods Manual*. Soil Survey Investigations Report No. 42, V. 3.0, National Soil Survey Center, Natural Resources Conservation Service, U.S. Department of Agriculture, Lincoln, NE.

Soil Survey Staff, 1999. Soil Taxonomy: A Basic System of Soil Classification for Making and Interpreting Soil Surveys, 2nd edition. Agriculture Handbook 436, Natural Resources Conservation Service, U.S. Department of Agriculture, Lincoln, NE.

Soriano, A., 1983. Deserts and semi-deserts of Patagonia. In: West, N.E. (Ed.), Temperate deserts and semi-deserts, Ecosystems of the World, vol. 5. Elsevier, Amsterdam, pp. 423–460.

Vogt, T., Larqué, P., 1998. Transformations and neoformations of clay in the cryogenic environment; examples from Transbaikalia (Siberia) and Patagonia (Argentina). European Journal of Soil Science 49, 367–376.

Zárate, M.A., 2003. Loess of southern South America. Quaternary Science Reviews 22, 1987–2006.